Reinforcement Learning-Based Integrated Control to Improve the Efficiency of DC Microgrids

Shivam Chaturvedi, *Member, IEEE*, Van-Hai Bui, *Member, IEEE*, Wencong Su, *Senior Member, IEEE*, and Mengqi Wang, *Senior Member, IEEE*

***Abstract*—The hierarchical control of the DC microgrid regulates the terminal voltages of the interfacing converter to achieve proportional load sharing and good voltage regulation at the DC bus. In doing so, the difference of the voltage at different nodes increases which results in higher circulating current and leads to higher losses. In this paper, a Reinforcement Learning Based Integrated Control (RLIC) is proposed which will minimize the circulating current and power losses in the transmission. The proposed RLIC consists of a primary and secondary controller. The primary controller is a robust sliding mode controller which receives the voltage references from secondary controller and regulates the terminal voltage and source current accordingly. The secondary control consists of a proportional integral control (PI), and a Deep Neural Network (DNN) surrogate model with implementation of Q-Learning as reinforcement method. A novel DNN based surrogate model uses the droop value from the PI controller and estimates the power loss and the local and global loading difference for a particular node, for a set of operating condition. This surrogate model is used by the Q-Learning based reinforcement technique which adjusts the droop constants and provide the voltage reference to primary controller to maintain load sharing and reduce the power losses, there-by leading to an improved overall efficiency. The proposed control structure is verified to improve efficiency while maintaining the load sharing and bus voltage regulation.**

***Index Terms*—DC microgrid, power management, droop control, dynamic droop control, proportional load sharing, artificial intelligence and DC microgrid, efficiency, energy distribution, DC microgrid operation, microgrid energy planning, Q-learning, surrogate model for DC microgrid, reinforcement learning in DC microgrid, machine learning in DC microgrid.**

I. Introduction

RECENTLY, there has been an increase in demand for an alternate method of energy generation to replace or support the conventional non-renewable sources of energy. The DC microgrids are considered as a viable solution in this aspect. A DC microgrid incorporates a photo-voltaic, fuel cell or wind turbine based source for energy generation. These sources are connected to a common bus by means of interfacing buck or a boost converter. These converters are used to regulate the DC bus voltage. A DC microgrid control usually consists of a hierarchical structure. It consists of a primary control which is responsible for local voltage and current regulations of a particular interfacing converter, a secondary control which is responsible to achieve characteristics like proportional load sharing among the source nodes, and a tertiary control which regulates a nodes as per the cost of energy generations. The hierarchical control is designed to achieve proportional load sharing and maintaining the DC bus voltage regulation during different load transitions [1]. In order to achieve proportional load sharing, the voltage reference to a node is varied such that if a source node is less loaded, its voltage reference to the primary controller is increased. On the other hand, if it is more loaded, the voltage reference must be reduced. The objective is to bring all the nodes in consensus for equal load sharing [2], [3]. In order to achieve the load sharing, different droop and dynamic droop methodologies have been proposed in literature. Droop control does not require any data exchange among the interfacing converter control nodes [4]. However, the droop value is to be calculated depending on the acceptable DC bus voltage regulation. Different dynamic droop based methodologies have been proposed in literature. A virtual resistance is proposed in [5] which is regulated based on the desired efficiency. Similar non-linear droop control is proposed in [6] to improve the load current sharing in microgrids. A secondary control with good voltage regulation is proposed in [7]. In [8], authors propose a low bandwidth communication in order to exchange the current and voltage values of nodes among the neighboring nodes. The local voltage and current values are compared with the communicated values and adequate changes in operating conditions are made. A team oriented load sharing method is proposed in [9], to improve load sharing and also reduce the circulating currents among the interfaced nodes. In [10], authors propose a control methodology which incorporates slope-adjusting approach to adjust the droop constant values as per the commands from the secondary control. Similarly, authors in [11], [12], [13] have proposed a scheme to improve the secondary control and plug and play operations. Different parallel computing methods have also been proposed to improve the microgrid dynamic performance [14], [15], [16]. However, these methodologies do not consider the distance of source nodes from the load nodes while assigning the droop constants. Under different loading conditions the droop constants can be assigned

Manuscript received 9 September 2022; revised 17 February 2023 and 8 May 2023; accepted 11 June 2023. Date of publication 16 June 2023; date of current version 26 December 2023. This work was supported in part by the U.S. National Science Foundation (NSF) under Award 2034938. Paper no. TSG-01337-2022. *(Corresponding author: Wencong Su.)*

The authors are with the Department of Electrical and Computer Engineering, University of Michigan-Dearborn, Dearborn, MI 48128 USA (e-mail: wencong@umich.edu).

Color versions of one or more figures in this article are available at https://doi.org/10.1109/TSG.2023.3286801.

Digital Object Identifier 10.1109/TSG.2023.3286801

such that, a high rated source node which is at farther distance from the load node can be more loaded than a less loaded node which is closer to the load node. This will inevitably result in a higher loss in transmission lines and reduce the overall efficiency of the microgrid system. On the other hand, if the references are further changed such that the droop is derived taking both the load sharing and transmission power efficiency, then a higher efficiency can be achieved.

Further, Reinforcement learning (RL) methodologies are being continuously used in different applications related to power conversions. The control methodologies for hybrid energy storage in microgrid has been proposed in [17], [18]. Deep reinforcement learning has been used for volts-var compensation in distribution systems in [19]. Agent based learning has also been applied for power flow solvers with volt-var compensation in [20]. Reinforcement methodologies has also been used to deriving an optimal power converter design in [21]. Hence, RL based methodologies are continuously finding applications in energy sector and these can be used to make the control scheme more optimal.

In this manuscript, a Reinforcement Learning based Integrated Control (RLIC) method is proposed to improve the efficiency of DC microgrid. The control is designed such that in low loading conditions, the load current is drawn from the sources which are closer to the load, while at higher loading conditions, the load current is drawn from the source nodes which have higher ratings. This leads to a dynamic variation of the voltage difference between the nodes, leading to better efficiency compared to traditional droop methodologies. The proposed RLIC consists of a sliding mode control based primary control and an integrated secondary control which consists of Proportional integral (PI) control, DNN surrogate model and Q-Learning algorithm. The sliding mode based primary control consists of dynamic surface which adapts according to the voltage and current conditions to achieve the reference obtained from the secondary controller. The secondary control of RLIC consist of PI control which provides the droop constants which will result in proportional load sharing among the nodes. This droop value is used by the DNN based surrogate model to predict the power loss and estimate the difference between the local node loading and the overall microgrid loading. The Q-Learning algorithm learns from the surrogate model and then dynamically varies the droop constants to achieve the desired objective of low losses while maintaining load sharing among the nodes. The output of the algorithm is the optimal droop which varies based on the desired objectives. The salient features of the proposed control are as follows:

1. The secondary control of the proposed RLIC ensures minimal losses by minimizing the voltage difference between the nodes. This leads to an improved efficiency.

2. The robust sliding mode based primary control of RLIC consists of dynamic surface, which ensures stability on a wide range of operating conditions.

3. The DNN based surrogate model is implemented to estimate the power losses and local and global current loading with respect to the droop values for individual nodes.

4. Proportional load sharing is maintained at high loading conditions, and distance based load sharing is achieved at low loading conditions.

The paper is organized as follows: Section II consists of derivation of the relation between the droop constant and power loss. Section III consists of modelling the boost converters connected to the microgrid. The derivation primary control law using the robust sliding mode control is presented in Sections IV and V. The stability of the proposed control is proved using the Lyapunov function is also presented in Section V. Integration of the PI control in secondary control is discussed in Section VI-A. Further, derivation of surrogate model and Q-Learning algorithm in presented in Sections VI-B and VI-C. These Sections also show corresponding waveform which verify the convergence to the required droop values. Finally, simulation results are shown in Section VII to verify the proposed control structure. Conclusion of the presented work and some future aspects are discussed in Section VIII.

II. Relation Between the Droop Constant and Power Loss

The droop control facilitates proportional load sharing by varying the voltage reference to a node in microgrid. The value of droop leads to some variation of a node voltage with respect to the DC bus voltage. Let us consider the DC bus voltage to be V_{dc}, the node voltage reference for i^{th} node to be V_{refi}, the droop constant for this node to be D_i and load current drawn from this node to be I_{Loadi}. The voltage reference for the i^{th} node can be derived as,

$$V_{refi} = V_{ref} - I_{Loadi} D_i \tag{1}$$

In the above equation, V_{ref} is the global desired reference of the DC bus voltage, which is common for all the nodes. The secondary control varies the voltage reference of a node to be less than or greater than this global reference voltage, depending on the loading condition for that particular node. Let's consider that the primary control of the node drives the voltage equal to the desired reference, then the load current drawn from the node can be derived as,

$$I_{Loadi} = \frac{V_{refi} - V_{dc}}{R_{Li}} \tag{2}$$

where, R_{Li} is the line resistance of the cable connecting the node to the DC bus. Substitute (1) in (2), and simplify to obtain (3),

$$I_{Loadi} = \frac{\left(V_{ref} - V_{dc}\right)}{(R_{Li} + D_i)} \tag{3}$$

The inverse relation between the node load current I_{Loadi} and the droop constant D_i can be observed from (3). Hence, higher the value of droop, lesser will be the load current drawn from the i^{th} node. The power loss occurs through the resistive component of the interfacing line which connects the node to the DC bus. Higher the difference between the node voltage and the DC bus voltage, higher will be the current and higher will be the power loss. The power loss (P_{Lossi}) in the

line connecting the i^{th} node to the common DC bus can be derived as,

$$P_{Lossi} = \left(\frac{V_{ref} - V_{dc}}{R_{Li} + D_i}\right)^2 R_{Li} \tag{4}$$

It can be observed from (4) that the power loss and droop constants are again inversely related. Hence, if the secondary control varies the droop constant value to maintain the proportional load sharing then it indirectly affects the power loss in the line interfacing the node to the DC bus. This will lead to degradation of the overall efficiency of the microgrid system.

III. Modeling of the DC Micro-Grid

The averaged model for i^{th} boost converter in a DC microgrid is derived as [22]:

$$L_i\dot{i}_{Li} = -r_{L_i}i_{Li} - (1-d_i)v_{ci} + V_{si} \tag{5}$$

$$C_i\dot{v}_{ci} = (1-d_i)i_{Li} - i_{oi} - \sum_{j\epsilon N_i} I_{ij} \tag{6}$$

where, N_i is the number of neighbors to the i^{th} converter, v_{ci} is the output voltage of converter across the capacitor C, i_{Li} is the current through the inductor L of the converter, V_{si} is the voltage of the source of i^{th} converter, r_{Li} is series resistance of the inductor L, i_{oi} is the output current of the converter, I_{ij} is the current between the node-i and node-j, and d_i the duty of i^{th} converter. Suppose the voltage and current references are V_i^{ref} and I_i^{ref} respectively, the voltage error E_{vi} and current error E_{ii} for i^{th} node can be derived as:

$$E_{ii} = i_{Li} - I_i^{ref}, \quad E_{vi} = v_{ci} - V_i^{ref} \tag{7}$$

Eq.(5) in error co-ordinates is derived as:

$$L_i\dot{E}_{ii} = -r_{L_i}\left(E_{ii} + I_i^{ref}\right) - u_i\left(E_{vi} + V_i^{ref}\right) + V_{si} \tag{8}$$

$$C_i\dot{E}_{vi} = u_i\left(E_{ii} + I_i^{ref}\right) - i_{oi} - \sum_{j\epsilon N_i} I_{ij} \tag{9}$$

where, $u_i = (1-d_i)$. The network topology can be represented by incidence matrix $B\epsilon \mathrm{IR}^{(N\times M)}$ where N is number of electrical nodes and M are the number of resistance edges between nodes. The overall dynamic model of DC microgrid in error co-ordinates will be:

$$L\dot{E}_i = -R\left(E_i + I^{ref}\right) - u * \left(E_v + V^{ref}\right) + V_s \tag{10}$$

$$C\dot{E}_v = u * \left(E_i + I^{ref}\right) - I_o - BR_L^{-1}B^T\left(E_v + V^{ref}\right) \tag{11}$$

where, '*' denotes Hadamard product and $L\epsilon \mathrm{IR}^{(N\times N)}$, $C\epsilon \mathrm{IR}^{(N\times N)}$, $R\epsilon \mathrm{IR}^{(N\times N)}$, $R_L\epsilon \mathrm{IR}^{(N\times N)}$ are positive definite diagonal matrices of inductor, capacitor, inductor resistances, and interfacing line resistance respectively. Also, $V_s\epsilon \mathrm{IR}^{(1\times N)}$, $E_i\epsilon \mathrm{IR}^{(1\times N)}$, $E_v\epsilon \mathrm{IR}^{(1\times N)}$, $I^{ref}\epsilon \mathrm{IR}^{(1\times N)}$, $u\epsilon \mathrm{IR}^{(1\times N)}$, $V^{ref}\epsilon \mathrm{IR}^{(1\times N)}$ are matrices of supply voltage, current error, voltage error, reference current, duty cycle difference from unity and reference voltage respectively.

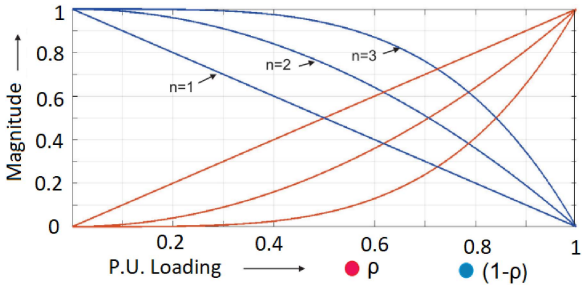

Fig. 1. Variation of ρ_i with p.u. loading of a converter.

IV. Proposed Current Reference Adjustment

The proposed control consists of two types of current references, a local reference and a global reference. The local reference is calculated by local voltage values while the global current reference is the mean of all the current supplied by the converters in the microgrid. Under low loading condition, the local reference is followed. While in high loading global loading will be followed. A constant ρ_i is used to smoothly vary the current reference.

$$I_{iL}^{ref} = \frac{V_i^{ref} i_{oi}}{V_{si}}, \quad I_{iG}^{ref} = \frac{\Sigma_{i=1}^{N} I_{iL}}{N} \tag{12}$$

where, I_{iL}^{ref} is the local current reference, I_{iL} is the per unit current of the i^{th} node, I_{iG}^{ref} is the global current reference, and N is the total number of nodes in microgrid. The overall current reference is given by:

$$I_i^{ref} = \rho_i I_{iG}^{ref} + (1-\rho_i) I_{i_L}^{ref} \tag{13}$$

The constant ρ_i depends on loading of i^{th} converter as:

$$\rho_i = (i_{Li}/I_{mi})^n \tag{14}$$

where n $\in \mathcal{R}^+$, and I_{mi} is the rated current of the interfacing converter. By choosing n, we can regulate the variation from local to global reference. The variation of ρ_i with respect to per-unit loading is shown in Fig. 1.

V. Proposed Robust Sliding Mode Control Based Primary Control Law

The primary control consists of a robust sliding mode control. The sliding manifold of the proposed control consists of the current and voltage error terms. The proposed sliding surface for i^{th} converter is:

$$s_i = \left(i_{Li} - I_i^{ref}\right) + \alpha_i\left(v_{ci} - V_i^{ref}\right) \tag{15}$$

where, $\alpha_i = \gamma_i E_{vi}^{\beta_i}$ and $I_i^{ref} = (\rho_i I_{iG}^{ref} + (1-\rho_i) I_{iL}^{ref})$. Hence, (15) I_i^{ref} is a combination of local and global current reference values. The constants α_i and $\gamma_i \in \mathcal{R}^+$ [23]. These two parameters are used to control voltage deviation within acceptable range when load variation occurs. The value of α_i varies when voltage deviation is above $\pm$ 5%, and it is negligible when voltage is within $\pm$ 5% range of the base voltage.

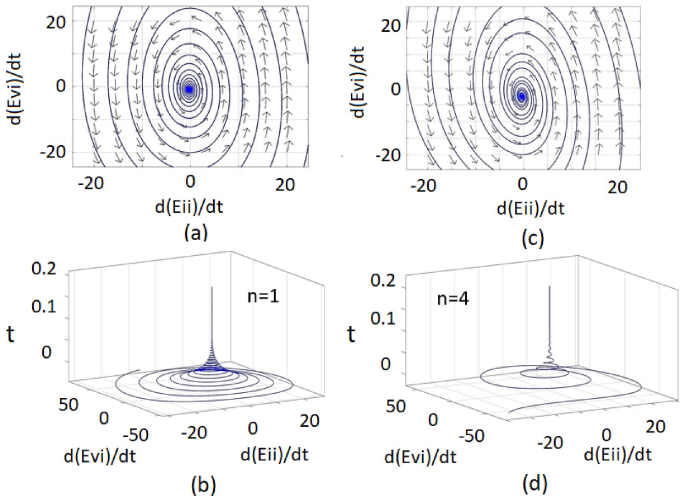

Fig. 2. Phase-plane plots for convergence of voltage and current errors (a) Phase plane for n=1, (b) Convergence with respect to time t in sec for n=1, (c) Phase plane for n=4, and (d) Convergence with respect to time for n=4.

A. Control Law

The proposed controller can be derived to obtain the reaching dynamics as [24]:

$$\dot{s_i} = -A_i s_i - B_i sign(s_i) \tag{16}$$

where, A_i and $B_i \in \mathrm{IR}^{(+)}$. Such dynamics would ensure that each converter's dynamics reach the sliding surface in finite time. By solving (8), (15) and (16) the control law can be derived to be:

$$u_i = \left(\frac{-\alpha_i\mu_i\left(I_{oi} + \sum I_{ij}\right) - \rho_i r_{Li}\left(E_{ii} + I_i^{ref}\right) + \rho_i V_{si}}{\rho_i\left(E_{vi} + V_i^{ref}\right) - \alpha_i\mu_i\left(E_{ii} + I_i^{ref}\right)}\right) + \left(\frac{L_i(A_i s_i + B_i sign(s_i))}{\rho_i\left(E_{vi} + V_i^{ref}\right) - \alpha_i\mu_i\left(E_{ii} + I_i^{ref}\right)}\right) \tag{17}$$

where, $\mu_i = \frac{L_i(\beta_i+1)}{C_i}$. From the above (17) it is observable that the branch currents affect the duty cycle but, these currents can be made limited by secondary control by choosing the voltage levels between two nodes.

B. Existence and Stability of Sliding Mode

Existence of sliding mode is guaranteed by η-reachability condition as [25]:

$$s_i\dot{s_i} < \eta|s_i| \qquad \eta > 0 \tag{18}$$

from (16),

$$s_i\dot{s_i} = s_i(-A_i s_i - B_i sgn(s_i))$$
$$s_i\dot{s_i} = (-A_i|s_i| - B_i)|s_i| \qquad s_i sign(s_i) = |s_i|$$

As, A_i and B_i are both chosen to be negative hence, $(-A_i|s_i| - B_i) < \eta$ and the dynamics will reach the designed sliding manifold. Stability of sliding mode is proved by Lyapunov stability. The convergence of the voltage error E_v will lead to convergence of the current error E_i and the current reference term depends on the voltage reference to a particular node. Hence, Lyapunov function will consists of E_v's and its convergence will be analysed. However, since we have multiple converters, there will be multiple functions each consisting of individual converters. For simplicity consider Lyapunov function for two converters:

$$V = \frac{E_{v1}^2}{2} + \frac{E_{v2}^2}{2} \tag{19}$$

On differentiating above with respect to time,

$$\dot{V} = \dot{E_{v1}}E_{v1} + \dot{E_{v2}}E_{v2} \tag{20}$$

For stability $\dot{V} < 0$ at all the operating conditions between two converter. From (9):

$$\dot{V} = \dot{V}_1 + \dot{V}_2 \tag{21}$$

where,

$$\dot{V}_1 = E_{v1}\left(\frac{1}{C_1}\left(u_1\left(E_{i1} + I_1^{ref}\right) - i_{o1} - \sum_{j\epsilon N} I_{1j}\right)\right)$$
$$\dot{V}_2 = E_{v2}\left(\frac{1}{C_2}\left(u_2\left(E_{i2} + I_2^{ref}\right) - i_{o2} - \sum_{j\epsilon N} I_{2j}\right)\right)$$

When the dynamics are at the sliding manifold, then s=0 which implies $E_{ii} = -\alpha_i E_{vi}$. The terms of $\dot{V}_1$ and $\dot{V}_2$ can be proved to be negative as in [23].

$$\dot{V_c} = -E_{v1}\sum_{j\epsilon N} I_{1j} - E_{v2}\sum_{j\epsilon N} I_{2j} \tag{22}$$

As we have two parallel connected converters, $I_{12} = -I_{21}$.

$$\dot{V_c} = -E_{v1}I_{12} - E_{v2}I_{21} \tag{23}$$
$$\dot{V_c} = I_{12}(E_{v2} - E_{v1}) \tag{24}$$

Substitute the value from (7) to obtain (25) as:

$$\dot{V_c} = I_{12}\left(V_1^{ref} - V_2^{ref}\right) \tag{25}$$

Consider the following cases:

Case 1: Branch current flows from node 2 to node 1. In this case I_{12} is positive and I_{21} is negative. This would happen if $V_2 > V_1$, which in turn would happen if $V_2^{ref} > V_1^{ref}$. This voltage reference is controlled by secondary dynamic consensus control. Hence, (25) will be negative definite.

Case 2: Similarly, if current flows from node 1 to node 2, I_{12} is negative definite and I_{21} is positive. This would happen if $V_1 > V_2$, which in turn would happen if $V_1^{ref} > V_2^{ref}$. Hence, (25) becomes,

$$\dot{V_c} = I_{12}\left(V_2^{ref} - V_1^{ref}\right) \tag{26}$$

This also remains negative definite.

Case 3: When there is no voltage difference between nodes then branch current is zero. Hence, $\dot{V_c}$ is zero. It can be observed that $\dot{V_c}$ is either negative of zero. This can be proved for all the converters in the microgrid. Hence, the system is stable. The convergence to zero voltage and current errors is shown in Fig. 2, for n=1 and n=4 with 80% loading. It can be seen that higher value of n will result in faster convergence. Convergence time for n=1 is about 0.08s while that for n=4 is less than 0.02s.

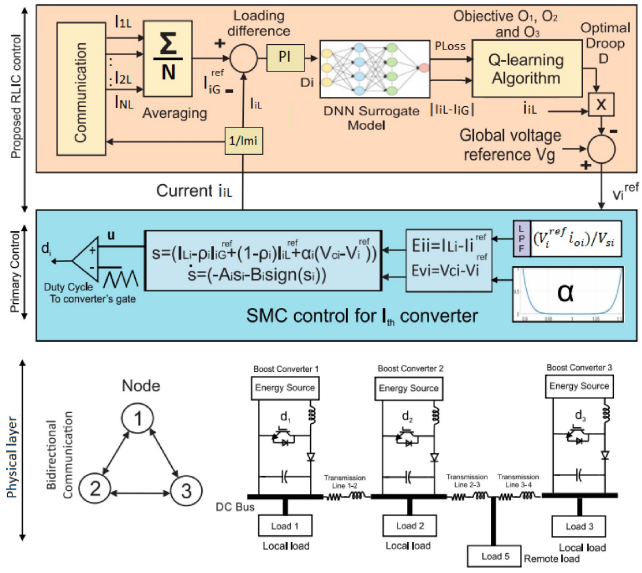

Fig. 3. Proposed RLIC control strategy with different layers of microgrid.

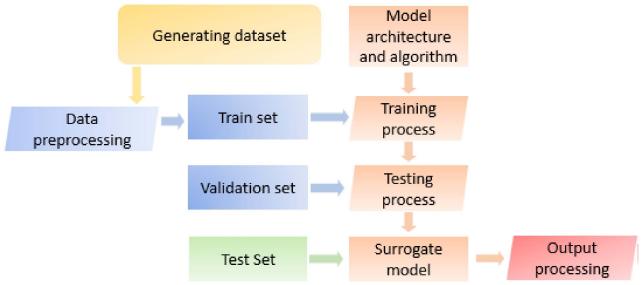

Fig. 4. Functional block diagram of the surrogate model, the data-set consists of the 75% train set, 15% validation set and 10% as test set.

TABLE I
METRICS FOR DNN SURROGATE EVALUATION

Parameters	Description
Input layer	Three Nodes for three Droop values
Output layer	Two Nodes for current difference and power losses
Two hidden layer	With 32 nodes/16 nodes
Activation function	RELU
Optimizer	Adam
Loss	MSE

VI. SECONDARY CONTROL

The secondary control consist of the proportional integral control, DNN surrogate model and Q-Learning algorithm. The per-unit current values from all the nodes are communicated and then processed by the proposed secondary control to derive the optimal droop constant which will result in minimal losses in the microgrid. Different sections of the proposed secondary control are discussed in the following sub-sections.

A. Proportional Integral Controller

The input to the PI control consists of the difference between the global loading reference and the local loading. The output of the PI control is the droop value which will result in reduction of the loading and make all the nodes share the load proportionally. The droop value D_i is obtained as:

$$D_i = \left(I_{iG}^{ref} - I_{iL}\right)\left(k_p + k_i/s\right) \tag{27}$$

The constants k_p and k_i are the proportional and integral gains of the PI controller. The global loading reference I_{iG}^{ref} is found by averaging the per-unit current quantities from the other nodes, i.e., $I_{iG}^{ref} = \sum_{i=1}^{N}(I_{iL}/N)$ as discussed earlier, and $I_{iL} = i_{Li}/I_{mi}$ such that I_{mi} is the maximum current that can be drawn from the i^{th} nodes. The droop D_i is usually given to the primary controller as in [26], [27], [28], but it results in significant power losses as discussed in previous sections. In order to make the droop optimal to achieve low power losses, the droop value is fed to the DNN surrogate model in order to estimate the power losses and the difference between the local and global loading, and then these values are used by the Q-Learning algorithm to derive the optimal droop, as shown in Fig. 3. The formulation of DNN surrogate model and Q-Learning algorithm is discussed in the following sections.

B. Derivation of Surrogate Model

The surrogate models are usually used to reduce the complexity, and computation of the system. Surrogate models are used where the output of a system is not easily measurable or when it takes a larger time for estimations, in the case of the DC microgrids [29]. In this work, a Deep-Neural Network (DNN) based surrogate model is used to estimate the difference between the actual loading and the average loading of the microgrid and also estimate the power loss.

1) Data-Set Generation: The proposed DNN based surrogate model consists of two stages, the first stage is data collection and the second phase is training, validation and testing of the DNN model, as shown in Fig. 4. During the first phase, a three node DC microgrid is simulated in MATLAB Simulink for different operating conditions and the corresponding quantities of interest such as the average microgrid loading, DC bus voltage, power loss estimation and different droop constant values are obtained. In total, 50,000 data samples are obtained to derive the DNN surrogate model. These data-sets are further divided in three data-sets used for training, validation and testing phases. The output of the surrogate model is further used by the Q-Learning algorithm to regulate the droop value.

2) Training and Testing of Surrogate Model: The DNN surrogate model is trained, validated and tested in order to estimate the output as close as possible to the actual simulation value. The metric on which the surrogate model in evaluated is shown in Table I. The 50,000 data-set obtained from simulation are further divided into three parts, which consists of 75% of data-set (i.e., train set with 37,500 samples), 15% of data-set (i.e., validation set with 7,500 samples), and 10% of data-set (i.e., test set with 5,000 samples). The methodology used for surrogate model is shown in Fig. 5. First the values which are to be fed to the DNN based surrogate model is normalized such that the maximum and minimum values of a parameter is mapped in the range of 0 to 1. These values are normalized within their maximum and minimum ranges such that droop ranges is considered from $[-8, 8]$, the O_1 range is taken between [0, 7] and the O_2 is taken between [0, 400e3]. The three parameters are generated randomly in

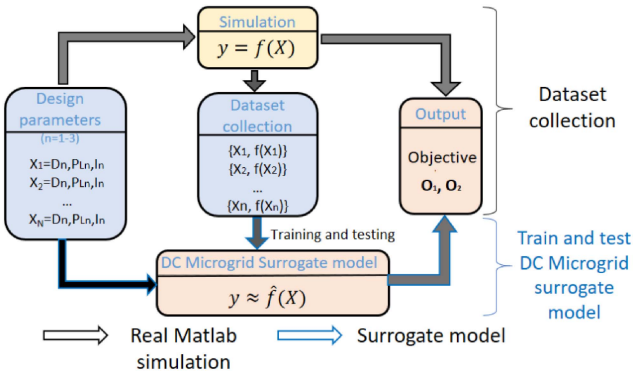

Fig. 5. Surrogate model derivation.

this range and the relation between all of them is derived through DNN. The parameters which are to be fed to the DNN model are the droop values, the difference of present loading to the global loading, and the estimated power loss. The DNN based surrogate model is trained when its output matches with the simulation result for the same input parameters. The output consist of the difference between the local and global loading and the total power loss. The training process of DNN is shown in Fig. 6 and for the loading condition and Fig. 7 for the total power loss. The Fig. 6a shows the loss with train set (75% of the total data-sets) and validation set (15% of the total data-sets). In order to test the accuracy of the proposed DNN surrogate model, 5,000 samples of test set (10% of the data-set) are used. The prediction error, which is the difference of the simulation and DNN output for O_1, remains within 0.3 and most of the times around zero, as can be seen from Fig. 6b. The actual and predicted values for test data-set inputs are shown in Fig. 6c. The prediction error is computed on the test set, as shown in Fig. 6d. It can be observed that the prediction error remains zero which represents a high co-relation between the simulated value of O_1 and the predicted value of O_1. Similarly, for objective O_2, the actual and predicted values for the test data-set shown in Fig. 7a. The prediction error for values of O_2 can be seen to be around zero which again signifies that there is negligible difference between the actual and predicted values, as shown in Fig. 7b. The actual and predicted values of O_2 for 5,000 samples of test set (10% of the data-set) are shown in Fig. 7c, showing that they are co-related. Finally, the frequency verses error plot is shown in Fig. 7d. Hence, the proposed DNN based surrogate model has been trained to provide the power loss estimation and the local and global loading difference for a particular droop value. This derived model is now used for secondary control support and also power loss reduction by manipulating the droop constant for a typical loading of a node in the microgrid network.

C. Implementation of Q-Learning Based Secondary Controller

The Q-Learning is a form of re-enforcement learning method which does not require intensive modelling of the environment or the plant [30]. It can be helpful for the case of DC microgrid as it consists of large amount of uncertainties in operation. The Q-Learning can handle different stochastic

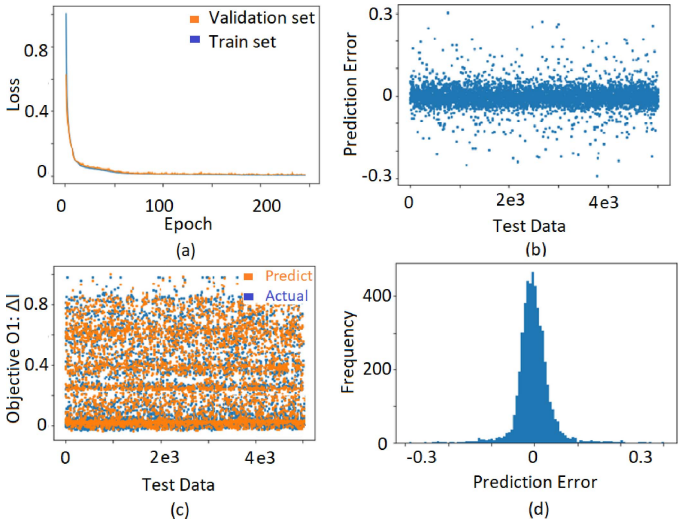

Fig. 6. DNN Surrogate model validation for Objective O_1, the data-set consists of the 75% train set, 15% validation set and 10% as test set.

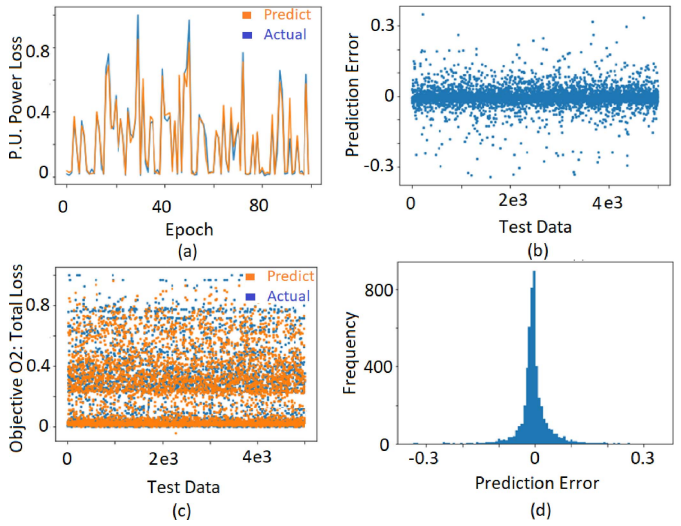

Fig. 7. DNN Surrogate model validation for Objective O_2, the data-set consists of the 75% train set, 15% validation set and 10% as test set.

based changes without the need of adaptations. It consist of a Q-table which will show the knowledge of a particular agent about its operating environment [31], [32]. The pair of a state and its action corresponds to a Q-value, which will signify how good or bad a particular action is. This is also termed as the reward of the action. A typical application of Q-Learning in the proposed methodology is shown in Fig. 8. The actions of Q-Learning algorithm consists of changing the droop values for all the three nodes and its corresponding output is the changes in the power loss and the local and global loading difference for all the nodes. The algorithm will compute the optimal droop values which results in minimal power loss with acceptable loading of all nodes. In the proposed methodology, the reward for a particular action is computed under three different case.

Case a: The first case consist of minimizing the difference between the local loading I_{iL} and global loading I_{iG} of every node. In this case, the power loss is not taken

Algorithm 1 Implemented Q-Learning Algorithm

Arbitrarily initialize Q(S,A), where S is present state and A is corresponding action

Repeat the following for every episode:

Initialize the state S

Select A from S using the Epsilon greedy policy

Perform action A and observe its corresponding response R and its new state S'

Update Q using, $Q(S,A) \leftarrow Q(S,A)+\beta[R+\gamma\ max_A\ Q(S',A')-Q(S,A)]$, $S \leftarrow S'$

where, γ is rate reward and β is the rate of learning

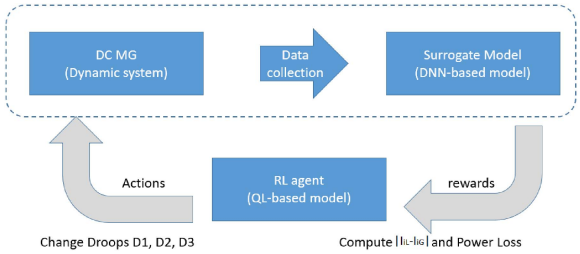

Fig. 8. Proposed Q-Learning algorithm with application to DC Microgrid.

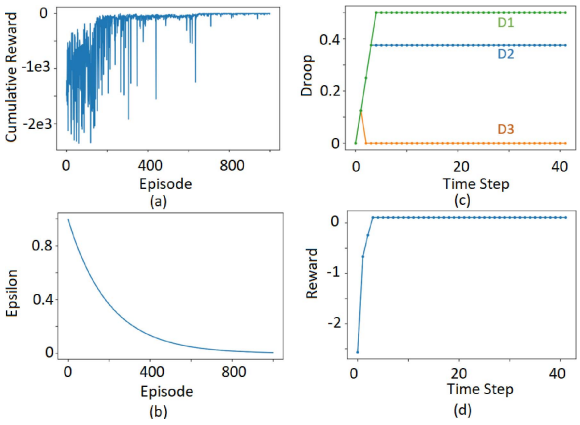

Fig. 9. Waveforms for achieving the minimization of objective O_1, (a) Cumulative reward, (b) Variation of epsilon with respect to the episodes, (c) Corresponding values of droops D_1, D_2, D_3 all the nodes, and (d) Minimization of reward function.

into consideration. The objective function O_1 taken into consideration is given as,

$$O_1 = \sum_{i=1}^{3} |I_{iL} - I_{iG}|. \tag{28}$$

In this objective, the agent varies the value of droop for large number of episodes and performs the actions such that the objective O_1 is minimized. The corresponding waveforms of cumulative reward, droop set points, epsilon and reward minimization's are shown in Fig. 9. It can be seen that three droop values are obtained which will lead to a minimal difference between the local and global loading set-points. These values are normalized and must be re-scaled between the $[-8, 8]$ value to attain the actual droop values. The value epsilon decides how a particular action is selected. Higher the value of epsilon, higher will be the random action of the

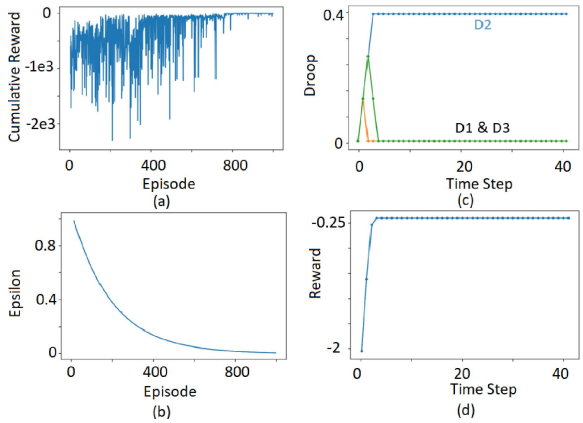

Fig. 10. Waveforms for achieving the minimization of objective O_2, (a) Cumulative reward, (b) Variation of epsilon with respect to the episodes, (c) Corresponding values of droops D_1, D_2, D_3 all the nodes, and (d) Minimization of reward function.

agent. As the value of epsilon reduces, the agent will become more and more knowledgeable about how to vary the droops to achieve the desired reduction of the objective.

Case b: In this case, the single objective is chosen which targets on minimizing the power loss. Hence, the action will converge towards having such a droop value for each of the node such that the power loss is minimal. The objective function O_2 is as follows:

$$O_2 = \sum_{i=1}^{3} |P_{Lossi}| \tag{29}$$

where, P_{Lossi} is the loss in the terminal connecting the node to the DC bus. This loss is to be minimized. Similar to the previous case, the waveforms corresponding the action and convergence to optimal droops which lead to minimal power loss is shown in Fig. 10.

Case c: Finally, a multi-objective reward function is chosen which consists of both minimizing of the global and local loading difference and also the power losses. The objective function consist of the summation of objectives O_1 and O_2. This will lead to a droop value which corresponds to a consensus in local and global loading and lesser power loss.

$$O_3 = \sum_{i=1}^{3} |I_{iL} - I_{iG}| + \sum_{i=1}^{3} |P_{Lossi}| \tag{30}$$

The corresponding waveforms are shown in Fig. 11. It can be inferred that the droop values will lead to minimal loss and minimal possible difference between the local and global loading. The overall proposed control with the primary and physical layers is shown in Fig. 3.

VII. Simulation Results

The proposed RLIC has been validate through a MATLAB simulation of a 4.5kW three node DC microgrid. The input voltages of source is 60V and the rated currents are (a) 40A for all nodes in all cases and, (b) 10A for nodes-1 and 2 and 40A for node-3 when testing for proportional load sharing. The line resistance between the nodes to the DC bus is

TABLE II
SIMULATION PARAMETERS

Symbol	Quantity	Value
V_{ref}, V_{dc}	Desired DC Bus Voltage	120V
V_s	Input Source Voltage	60V
L	Inductance of the converter	2mH
C	Capacitance of converter	$100\mu F$
R_{Li} (i=1,3)	Line resistances for node-1,2 and 3	$1\Omega, 2\Omega, 3\Omega$
A_i, B_i	Sliding mode reaching dynamics	17000, 2000
β_i, η_i	Surface parameters	6, 10^{-8}

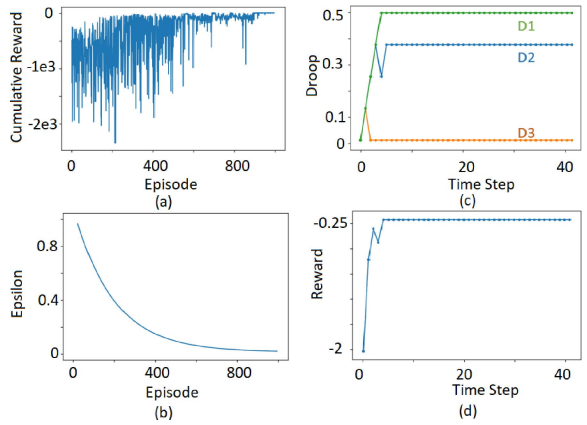

Fig. 11. Waveforms for achieving the minimization of objective O_3, (a) Cumulative reward, (b) Variation of epsilon with respect to the episodes, (c) Corresponding values of droops D_1, D_2, D_3 all the nodes, and (d) Minimization of reward function.

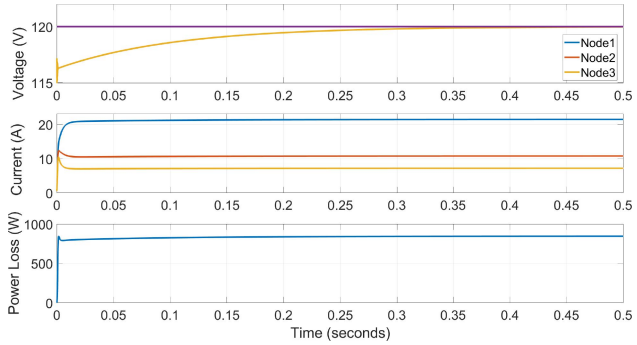

Fig. 12. Waveforms without droop control, $R_{Load} = 5\Omega$.

1Ω, 2Ω and 3Ω for nodes -1, 2 and 3 respectively. The primary control consist of a robust sliding mode control and the secondary control consists of the integrated proportional integral control assisted by the DNN surrogate and Q learning algorithm. The simulation results has been classified into the following subsections.

A. Without Droop and Secondary Control

The voltage, current and power loss waveforms has been shown in Fig. 12. It can be seen that in the absence of any droop, the voltage of DC bus remains 120V, but the current is not shared proportionally. It can be seen that the node-1 is more loaded compared to the nodes-2 and 3. The total power loss is about 750W as the terminal voltage of all nodes is the same.

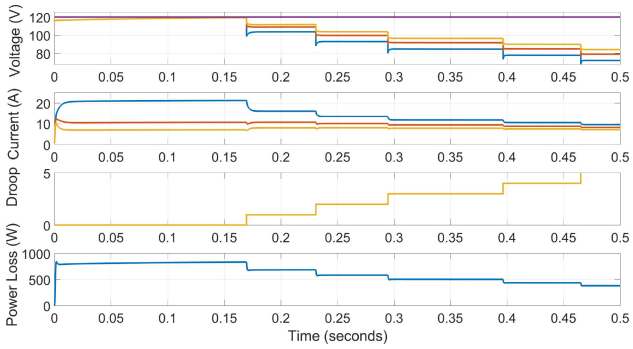

Fig. 13. Waveforms with constant droop in all nodes: Droop increased simultaneously, and DC bus voltage degrades.

B. With Constant Droop in All the Nodes

In order to achieve equal load sharing, the droop at all the nodes is increased simultaneously. The higher the droop constant, more proportional can be the load sharing at the cost of degrading DC bus voltage, as can be observed from Fig. 13. The power loss also reduces because of the terminal DC bus voltage reduction. The degradation of the DC bus voltage puts a limit to the droop value used.

C. Dynamic Droop Control and All Nodes Are of Same Rating

In this case, the proportional integral secondary control is implemented to regulate the droop values. Hence, the value of droop constants can either be positive or negative. The secondary control is activated after T=0.125s. Hence, the load sharing becomes equal and the terminal voltage change due to dynamic droop as shown in Fig. 14. But it should also be seen that the losses increases from about 800W initially to 960W. This is about 20% more losses compared to the implementation without dynamic droop.

D. Dynamic Droop With the Farther Node Is Higher Rating

The losses further increase if we consider that the node which is farther from the load has higher rating. In this case, the farther node has to provide more current, for proportional load sharing and this will cause an increase of losses. In this case we consider that the Node-3 is 2.5kW while nodes 1 and 2 are 600W. The increase in losses are shown in Fig. 15.

Case a (Optimized droop for equal load sharing-O_1): The proposed control is implemented with optimized droops to achieve equal load sharing. The currents from all the nodes are almost the same. The highly loaded node becomes less loaded and the load of node-3 is increased. The corresponding waveforms are shown in Fig. 16. It can be observed that the current from each node is about 12A and the power loss is 825W.

Case b (Optimized droop for least power loss-Objective O_2): The objective O_2 is to achieve least power loss during power distribution. This is achieved by the proposed control by making the Q-Learning algorithm's objective to minimize O_2. The waveforms are shown in Fig. 17. It must be observed that

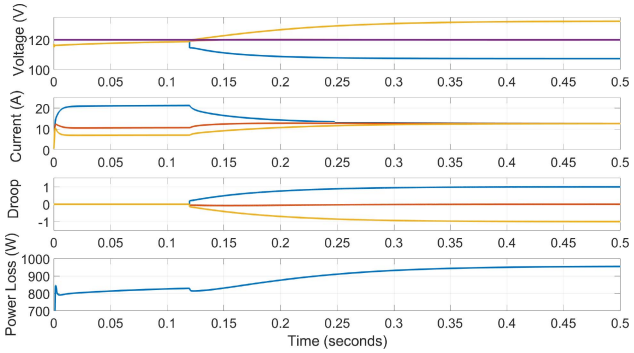

Fig. 14. Waveforms with consensus based droop control for all nodes: Control implemented after t=0.12s, the currents are shared equally but power loss increases, $R_{Load} = 5\Omega$.

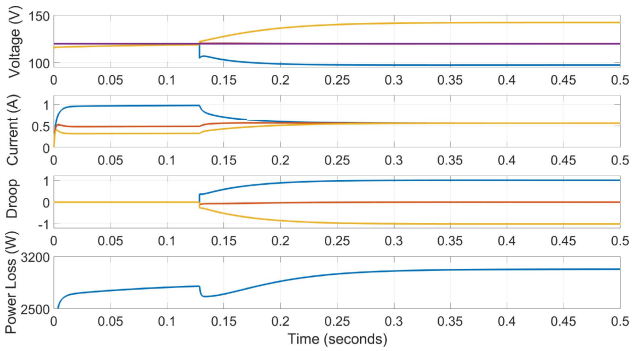

Fig. 15. Waveforms with different source ratings: Node-1 and 2 are rated at 600W and Node-3 is rated at 2400W. Node-3 has highest rating but the line connecting it to DC bus has highest resistance, hence highest loss, dynamic control implemented at t=0.12s, $R_{Load} = 30\Omega$.

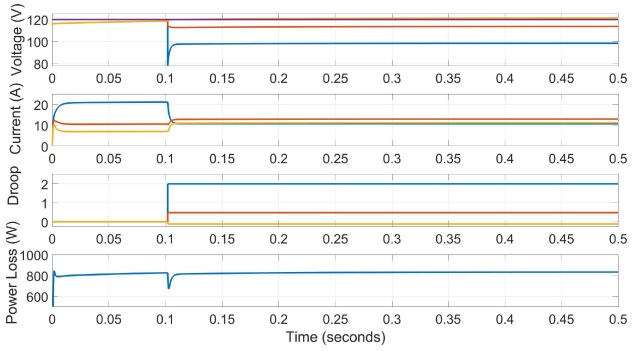

Fig. 16. Waveforms for Case a, optimized droop to achieve objective O_1, RLIC implemented at t=0.1s, $R_{Load} = 5\Omega$.

the power loss is the least among all the simulation have conducted so far, which is about 700W. Now, in order to achieve load sharing along with minimal power loss, the objective O_3 is used.

Case c (Optimized droop for equal load sharing and reduced power loss-Objective O_3): This is the simulation for case c. In this, the objective for Q-Learning is O_3, which is reduced loss and improved load sharing. The simulation waveforms are shown in Fig. 18. It must be observed that the load sharing is improved than case b, and losses have reduced than case-a. The current from node-1 is 14A, from node-2 is 13A and from node-3 is 10A. The power loss is 760W.

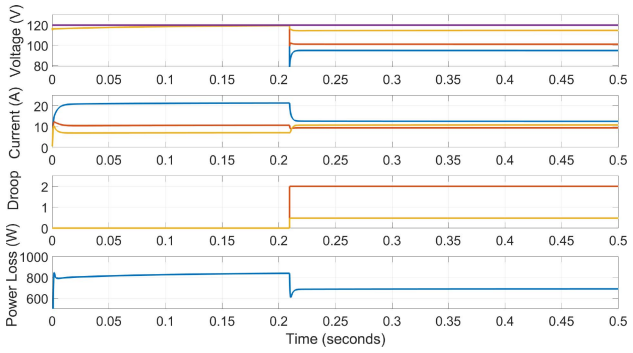

Fig. 17. Waveforms for Case b, optimized droop to achieve objective O_2-least power loss, minimal power loss must be observed, RLIC implemented at t=0.2s, $R_{Load} = 5\Omega$.

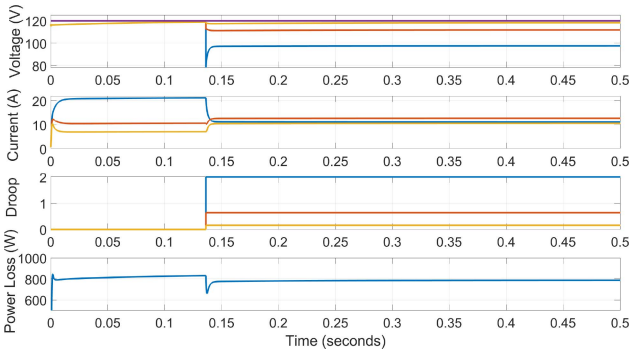

Fig. 18. Waveforms for Case c, optimized droop to achieve objective O_3-less power loss with improved load sharing, power loss lesser than case a. RLIC implemented at t=0.12s, $R_{Load} = 5\Omega$.

Hence, depending on the usage, the objective function can be chosen. The proposed control has been proved to reduce the distribution power loss while maintaining load sharing the DC microgrids. A comparison of the proposed RLIC with different other methods in literature is presented in Table III.

VIII. Conclusion

The efficiency of DC microgrid largely depends on the droop constants as it leads to different node voltages which leads to circulating currents among the nodes. In order to reduce the losses, a RLIC has been proposed which consists of a DNN based surrogate model to mimic the behavior of global nodes, and Q-Learning algorithm which optimizes the values of droop constants to the node. This integrated secondary control provides reference to the proposed robust sliding mode control based primary control, which is robust and drives the nodes to desired voltage reference. Several cases have been verified and it can be concluded that the power loss reduces significantly from 970W to 760W for the same operating conditions. Hence, the power loss of about 210W is mitigated, which is about 21% reduction of losses. Hence, the proposed RLIC has been proved to be effective in improving the efficiency of the microgrid as a whole. As a future work, the proposed control can be extended to switch between the optimized droop and consensus based droop value based on the loading and the DC bus voltage regulation conditions.

TABLE III
COMPARISON

Parameter	[33]	[34]	[35]	[36]	Proposed RLIC
Primary Controller	Droop based Sliding Mode Controller	Multi-Objective Droop	Dual-Loop Proportional Integral	PI control and Droop	Robust Sliding mode control
Secondary Controller	Not available	No	Proportional Integral	Consensus Control	Q-Learning
Distribution efficiency	Not considered	Degrades with loading	Degrades with loading	Not estimated	Highly improved
Node voltage difference	Increases with loading	Increases depending on droop gains	Increases as an average of the microgrid cluster	Will increase with loading	Varied to get the best efficiency
Proportional load sharing	Not achieved	Achieved	Achieved	Achieved	Achieved during peak loading conditions
Ease of implementation	Easier- no communication	Challenging to keep good voltage regulation	Complex to tune secondary control when the number of node increases	Designing consensus control can be complex when scaled up	Easy deployment to existing systems.

ACKNOWLEDGMENT

The authors also would like to thank the anonymous editors and reviewers for their valuable comments and suggestions to improve the quality of this paper. Any opinions, findings, conclusions, or recommendations expressed in this material are those of the author(s) and do not necessarily reflect the views of the National Science Foundation.

REFERENCES

[1] T. Dragičević, X. Lu, J. C. Vasquez, and J. M. Guerrero, "DC Microgrids—Part I: A review of control strategies and stabilization techniques," *IEEE Trans. Power Electron.*, vol. 31, no. 7, pp. 4876–4891, Jul. 2016.

[2] S. Chaturvedi and D. Fulwani, "Adaptive voltage tuning based load sharing in DC microgrid," *IEEE Trans. Ind. Appl.*, vol. 57, no. 1, pp. 977–986, Jan./Feb. 2021.

[3] V.-V. Thanh and W. Su, "Improving current sharing and voltage regulation for DC microgrids: A decentralized demand response approach," *IEEE Trans. Smart Grid*, vol. 14, no. 4, pp. 2508–2520, Jul. 2023.

[4] T. Dragičević, X. Lu, J. C. Vasquez, and J. M. Guerrero, "DC Microgrids—Part II: A review of power architectures, applications, and standardization issues," *IEEE Trans. Power Electron.*, vol. 31, no. 5, pp. 3528–3549, May 2016.

[5] L. Meng, T. Dragicevic, J. C. Vasquez, and J. M. Guerrero, "Tertiary and secondary control levels for efficiency optimization and system damping in droop controlled DC–DC converters," *IEEE Trans. Smart Grid*, vol. 6, no. 6, pp. 2615–2626, Nov. 2015.

[6] X. Feng, K. L. Butler-Purry, and T. Zourntos, "Multi-agent system-based real-time load management for all-electric ship power systems in DC zone level," *IEEE Trans. Power Syst.*, vol. 27, no. 4, pp. 1719–1728, Nov. 2012.

[7] K. Sun, L. Zhang, Y. Xing, and J. M. Guerrero, "A distributed control strategy based on DC bus signaling for modular photovoltaic generation systems with battery energy storage," *IEEE Trans. Power Electron.*, vol. 26, no. 10, pp. 3032–3045, Oct. 2011.

[8] X. Lu, J. M. Guerrero, K. Sun, and J. C. Vasquez, "An improved droop control method for DC Microgrids based on low bandwidth communication with DC bus voltage restoration and enhanced current sharing accuracy," *IEEE Trans. Power Electron.*, vol. 29, no. 4, pp. 1800–1812, Apr. 2014.

[9] S. Moayedi, V. Nasirian, F. L. Lewis, and A. Davoudi, "Team-oriented load sharing in parallel DC–DC converters," *IEEE Trans. Ind. Appl.*, vol. 51, no. 1, pp. 479–490, Jan./Feb. 2015.

[10] D.-H. Dam and H.-H. Lee, "A power distributed control method for proportional load power sharing and bus voltage restoration in a DC microgrid," *IEEE Trans. Ind. Appl.*, vol. 54, no. 4, pp. 3616–3625, Jul./Aug. 2018.

[11] J. W. Simpson-Porco, Q. Shafiee, F. Dörfler, J. C. Vasquez, J. M. Guerrero, and F. Bullo, "Secondary frequency and voltage control of Islanded Microgrids via distributed averaging," *IEEE Trans. Ind. Electron.*, vol. 62, no. 11, pp. 7025–7038, Nov. 2015.

[12] M. Tucci, S. Riverso, and G. Ferrari-Trecate, "Line-independent plug-and-play controllers for voltage stabilization in DC microgrids," *IEEE Trans. Control Syst. Technol.*, vol. 26, no. 3, pp. 1115–1123, May 2018.

[13] V.-V. Thanh, W. Su, and B. Wang, "Optimal DC Microgrid operation with model predictive control-based voltage-dependent demand response and optimal battery dispatch," *Energies*, vol. 15, no. 6, p. 2140, 2022. [Online]. Available: https://www.mdpi.com/1996-1073/15/6/2140

[14] A. Mondal, S. Misra, and M. S. Obaidat, "Distributed home energy management system with storage in smart grid using game theory," *IEEE Syst. J.*, vol. 11, no. 3, pp. 1857–1866, Sep. 2017.

[15] W. Shi, X. Xie, C.-C. Chu, and R. Gadh, "Distributed optimal energy management in microgrids," *IEEE Trans. Smart Grid*, vol. 6, no. 3, pp. 1137–1146, May 2015.

[16] F. Chang, X. Cui, M. Wang, and W. Su, "Region of attraction estimation for DC Microgrids with constant power loads using potential theory," *IEEE Trans. Smart Grid*, vol. 12, no. 5, pp. 3793–3808, Sep. 2021.

[17] J. Duan, Z. Yi, D. Shi, C. Lin, X. Lu, and Z. Wang, "Reinforcement-learning-based optimal control of hybrid energy storage systems in hybrid AC–DC microgrids," *IEEE Trans. Ind. Informat.*, vol. 15, no. 9, pp. 5355–5364, Sep. 2019.

[18] X. Zhang, B. Wang, D. Gamage, and A. Ukil, "Model predictive and iterative learning control based hybrid control method for hybrid energy storage system," *IEEE Trans. Sustain. Energy*, vol. 12, no. 4, pp. 2146–2158, Oct. 2021.

[19] Y. Zhang, X. Wang, J. Wang, and Y. Zhang, "Deep reinforcement learning based volt-VAR optimization in smart distribution systems," *IEEE Trans. Smart Grid*, vol. 12, no. 1, pp. 361–371, Jan. 2021.

[20] X. Zhang, A. J. Flueck, and C. P. Nguyen, "Agent-based distributed volt/Var control with distributed power flow solver in smart grid," *IEEE Trans. Smart Grid*, vol. 7, no. 2, pp. 600–607, Mar. 2016.

[21] V.-H. Bui et al., "Deep neural network-based surrogate model for optimal component sizing of power converters using deep reinforcement learning," *IEEE Access*, vol. 10, pp. 78702–78712, 2022.

[22] S. Chaturvedi, D. Fulwani, and J. M. Guerrero, "Adaptive-SMC based output impedance shaping in DC Microgrids affected by inverter loads," *IEEE Trans. Sustain. Energy*, vol. 11, no. 4, pp. 2940–2949, Oct. 2020.

[23] A. R. Gautam, K. Gourav, J. M. Guerrero, and D. M. Fulwani, "Ripple mitigation with improved line-load transients response in a two-stage DC–DC–AC converter: Adaptive SMC approach," *IEEE Trans. Ind. Electron.*, vol. 65, no. 4, pp. 3125–3135, Apr. 2018.

[24] V. I. Utkin, J. Guldner, and J. Shi, *Sliding Mode Control in Electromechanical Systems*. Abington Township, PA, USA: Taylor Francis, 1999.

[25] C. Edwards and S. Spurgeon, *Sliding Mode Control: Theory and Applications*. Boca Raton, FL, USA: CRC Press, 1998.

[26] S. Anand, B. G. Fernandes, and J. Guerrero, "Distributed control to ensure proportional load sharing and improve voltage regulation in low-voltage DC microgrids," *IEEE Trans. Power Electron.*, vol. 28, no. 4, pp. 1900–1913, Apr. 2013.

[27] S. Chaturvedi, D. Fulwani, and D. Patel, "Dynamic virtual impedance-based second-order ripple regulation in DC microgrids," *IEEE J. Emerg. Sel. Topics Power Electron.*, vol. 10, no. 1, pp. 1075–1083, Feb. 2022.
[28] V. Nasirian, S. Moayedi, A. Davoudi, and F. L. Lewis, "Distributed cooperative control of DC microgrids," *IEEE Trans. Power Electron.*, vol. 30, no. 4, pp. 2288–2303, Apr. 2015.
[29] A. Bhosekar and M. Ierapetritou, "Advances in surrogate based modeling, feasibility analysis, and optimization: A review," *Comput. Chem. Eng.*, vol. 108, pp. 250–267, Jan. 2018. [Online]. Available: https://www.sciencedirect.com/science/article/pii/S0098135417303228
[30] V.-H. Bui, A. Hussain, and H.-M. Kim, "Double deep *Q*-learning-based distributed operation of battery energy storage system considering uncertainties," *IEEE Trans. Smart Grid*, vol. 11, no. 1, pp. 457–469, Jan. 2020.
[31] M. Zhao, X. Li, L. Gao, L. Wang, and M. Xiao, "An improved Q-learning based rescheduling method for flexible job-shops with machine failures," in *Proc. IEEE 15th Int. Conf. Autom. Sci. Eng. (CASE)*, 2019, pp. 331–337.
[32] K.-Y. Chou, Y.-T. Chen, J.-K. Lin, S.-L. Ho, and Y.-P. Chen, "Q-learning based tracking control and slope climbing strategy design of autonomous mobile robot and flatbed vehicle," in *Proc. IEEE Int. Conf. Consum. Electron. Taiwan (ICCE-TW)*, 2021, pp. 1–2.
[33] M. Veysi, J. Aghaei, M. R. Soltanpour, M. Shasadeghi, B. Bahrani, and D. J. Ryan, "Robust, accurate, and fast decentralized power sharing mechanism for isolated DC microgrid using droop-based sliding-mode control," *IEEE Trans. Smart Grid*, vol. 13, no. 6, pp. 4160–4173, Nov. 2022.
[34] A. M. Dissanayake and N. C. Ekneligoda, "Multiobjective optimization of droop-controlled distributed generators in DC microgrids," *IEEE Trans. Ind. Informat.*, vol. 16, no. 4, pp. 2423–2435, Apr. 2020.
[35] R. Babazadeh-Dizaji, M. Hamzeh, and K. Sheshyekani, "A consensus-based cooperative control for DC microgrids interlinked via multiple converters," *IEEE Syst. J.*, vol. 15, no. 4, pp. 4918–4926, Dec. 2021.
[36] W. Jiang, C. Yang, Z. Liu, M. Liang, P. Li, and G. Zhou, "A hierarchical control structure for distributed energy storage system in DC microgrid," *IEEE Access*, vol. 7, pp. 128787–128795, 2019.

Shivam Chaturvedi (Member, IEEE) received the B.Tech. degree in electrical and electronics engineering from Uttar Pradesh Technical University, Lucknow, India, in 2013, the M.E. degree in power electronics from the Shri Govindram Seksaria Institute of Technology, Indore, India, in 2015, and the Ph.D. degree in area of power electronics from the Indian Institute of Technology Jodhpur, India, in 2021. He is currently working as a Research Investigator with the Department of Electrical and Computer Engineering, University of Michigan-Dearborn, MI, USA. His research interests include dc and ac microgrids control, virtual impedance shaping, dc–ac power electronic interfaces, high power density converters, electric vehicle battery charging methodologies, and electric vehicle traction inverter control design.

Van-Hai Bui (Member, IEEE) received the B.E. degree in electrical engineering from the Hanoi University of Science and Technology, Vietnam, in 2013, and the Ph.D. degree in electrical engineering from Incheon National University, South Korea, in 2020. He was an Assistant Professor with the Department of Electrical Engineering, State University of New York, Maritime College, USA, from 2022 to 2023. Since August 2023, he has been an Assistant Professor with the Department of Electrical and Computer Engineering, University of Michigan-Dearborn, USA. His research interests include energy management systems, applications of machine learning in smart grids, operation and control of power and energy systems.

Wencong Su (Senior Member, IEEE) received the B.S. degree (with distinction) from Clarkson University, Potsdam, NY, USA, in 2008, the M.S. degree from Virginia Tech, Blacksburg, VA, USA, in 2009, and the Ph.D. degree from North Carolina State University, Raleigh, NC, USA, in 2013. He is currently a Professor and the Department Chair of Electrical and Computer Engineering with the University of Michigan-Dearborn, USA. His research interests include power systems, transportation electrification, machine learning applications, and cyber-physical systems. He received the 2015 IEEE Power and Energy Society Technical Committee Prize Paper Award and the 2013 IEEE Industrial Electronics Society Student Best Paper Award. He is an Editor for the IEEE TRANSACTIONS ON SMART GRID and IEEE POWER ENGINEERING LETTERS, an Associate Editor for the IEEE ACCESS and IEEE DataPort, and a Fellow of IET.

Mengqi Wang (Senior Member, IEEE) received the B.S. degree in electrical engineering from Xi'an Jiaotong University, Xi'an, China, in 2009, and the Ph.D. degree in electrical engineering from North Carolina State University, Raleigh, NC, USA, in 2014. She is currently an Associate Professor with the Department of Electrical and Computer Engineering, University of Michigan-Dearborn, Dearborn, MI, USA. Her research interests include dc–dc and dc–ac power conversions, high-efficiency and high-power-density power supplies, renewable energy systems, and wide-bandgap power device applications.